Nuclear Technology

ISSN: 0029-5450 (Print) 1943-7471 (Online) Journal homepage: www.tandfonline.com/journals/unct20

Experimental Study on Flow Optimization in Upper Plenum of Reactor Vessel for a Compact Sodium-Cooled Fast Reactor

Nobuyuki Kimura, Kenji Hayashi, Hideki Kamide, Masami Itoh & Tadashi Sekine

To cite this article: Nobuyuki Kimura, Kenji Hayashi, Hideki Kamide, Masami Itoh & Tadashi Sekine (2005) Experimental Study on Flow Optimization in Upper Plenum of Reactor Vessel for a Compact Sodium-Cooled Fast Reactor, Nuclear Technology, 152:2, 210-222, DOI: 10.13182/NT05-A3671

To link to this article: https://doi.org/10.13182/NT05-A3671

Published online: 10 Apr 2017.

EXPERIMENTAL STUDY ON FLOW OPTIMIZATION IN UPPER PLENUM OF REACTOR VESSEL FOR A COMPACT SODIUM-COOLED FAST REACTOR

THERMAL HYDRAULICS

KEYWORDS: *gas entrainment, fast reactor, particle image velocimetry*

NOBUYUKI KIMURA,* KENJI HAYASHI, and HIDEKI KAMIDE
Japan Nuclear Cycle Development Institute, O-arai Engineering Center
4002 Narita, O-arai, Ibaraki 311-1393, Japan

MASAMI ITOH and TADASHI SEKINE *Joyo Industry Co. Ltd.*
1141-4, Muramatsu, Tokai, Ibaraki 319-1112, Japan

Received August 3, 2004
Accepted for Publication November 1, 2004

An innovative sodium-cooled fast reactor has been investigated in a feasibility study of fast breeder reactor cycle systems in Japan. A compact reactor vessel and a column-type upper inner structure with a radial slit for an arm of a fuel-handling machine (FHM) are adopted. Dipped plates are set in the reactor vessel below the free surface to prevent gas entrainment. We performed a one-tenth–scaled model water experiment for the upper plenum of the reactor vessel. Gas entrainment was not observed in the experiment under the same velocity condition as the reactor. Three vortex cavitations were observed near the hot-leg inlet. A vertical rib on the reactor vessel wall was set to restrict the rotating flow near the hot leg. The vortex cavitation between the reactor vessel wall and the hot leg was suppressed by the rib under the same cavitation factor condition as in the reactor. The cylindrical plug was installed through the hole in the dipped plates for the FHM to reduce the flow toward the free surface. It was effective when the plug was submerged into the middle height in the upper plenum. This combination of two components had a possibility to optimize the flow in the compact reactor vessel.

I. INTRODUCTION

In fast reactors, improving cost performance is as important as safety. At the Japan Nuclear Cycle Development Institute, various types of fast reactors have been investigated in a feasibility study of fast reactor cycle systems since 1999 (Ref. 1). One of the significant options is an advanced loop–type sodium-cooled fast reactor with a 1500-MW(electric) class core.[2] A design study is under way for this plant. The reactor system is simplified to reduce construction cost so as to compete with a future commercial light water reactor and to maintain safety. For example, thermal output increases against the reactor size, an intermediate heat exchanger (IHX) and a main primary pump are united, the number of primary loops decreases from three or four to two, and so on. As for the upper plenum of a reactor vessel, a single rotation plug and a fuel-handling machine (FHM) with a swing-type arm are adopted to simplify the fuel-handling system. A column-type upper inner structure (UIS), which consists of control rod guide tubes and six horizontal perforated plates and has no outer cover, has a radial slit in the horizontal plates for the arm of the FHM to move inside the UIS and access all subassemblies. The diameter of the reactor vessel can be reduced by using this UIS concept with the slit. There is no need for space to move out the UIS from the core top during fuel handling. Coolant passes through the inside of the UIS to increase mixing volume in the upper plenum and to mitigate thermal transient after a scram. There is a free surface in the upper plenum of the reactor vessel to keep a deck at lower temperature. As compared with the Japanese Demonstration Fast Breeder Reactor (FBR) of 600-MW(electric) class (design study),[3] core flow rate increases as thermal output increases by factor of 2.5, while the diameter of the reactor vessel is nearly equal. These result in an increase of the spatial-averaged velocity on the horizontal cross section of the reactor vessel by a factor of 2.5. This large amount of coolant is sucked into two

*E-mail: kimura@oec.jnc.go.jp

hot-leg intakes; the average velocity in the hot-leg pipe reaches 9.2 m/s. Further, the slit of the UIS permits local high velocity from the core outlet toward the free surface. These high velocities may cause gas entrainment at the free surface in the upper plenum and the cavitations. Therefore, horizontal dipped plates are set up below the free surface to prevent the gas entrainment. Cover gas above the free surface is pressurized at 0.25 MPa (absolute pressure) on a point of cavitations because of high velocity. However, there are many gaps between the dipped plates and the hot-leg pipes and between the dipped plates and the reactor vessel, etc. The flow velocity passing through the UIS slit is comparable with core outlet velocity, ~5 m/s, and this flow collides with the dipped plates.

In the study on the gas entrainment in the IHX vessel for the Japanese Demonstration FBR (Ref. 4), water experiments were carried out using four scaled models from one-tenth to 1/1.6 scale. Dependence of the scale and the velocity condition were estimated for the onset of the gas entrainment. Furthermore, it was shown that the flow pattern in the IHX was independent of the Reynolds number. In addition, onset condition of gas entrainment in sodium was compared with water, including the influence of fluid property.[5] It was shown that the onset condition of gas entrainment depended on the Weber number. The surface tension of sodium was larger than that of water. Therefore, it was found that water experiments were conservative to sodium.

We performed a one-tenth–scaled model water experiment for the upper plenum in the reactor vessel. The objective of the study is flow optimization in the upper plenum to have prospects of this compact reactor vessel. Flow fields in the upper plenum are evaluated by using visualization, the particle image velocimetry[6] (PIV), and the ultrasound velocity profile (UVP) monitor.[7] This quantification of flow fields enables us to optimize the flow based on the phenomenalism. And other hydraulic problems are also picked up. After that, we investigate suitable structures to control the flow in the upper plenum.

II. EXPERIMENT

II.A. Design of an Advanced Loop–Type Sodium-Cooled Fast Reactor

Figure 1 shows a reactor vessel of an advanced loop–type sodium-cooled fast reactor in the design phase at the end of fiscal 2001. The diameter of the core is 6580 mm, and the inner diameter of the reactor vessel is 9700 mm. The primary cooling system consists of two loops, and each loop has one hot-leg pipe and two cold-leg pipes in the upper plenum of the reactor vessel. These two hot-leg pipes and four cold-leg pipes are put into the upper plenum from the top. In addition, two cold traps, which purify sodium, and a dipped heat exchanger (DHX), which

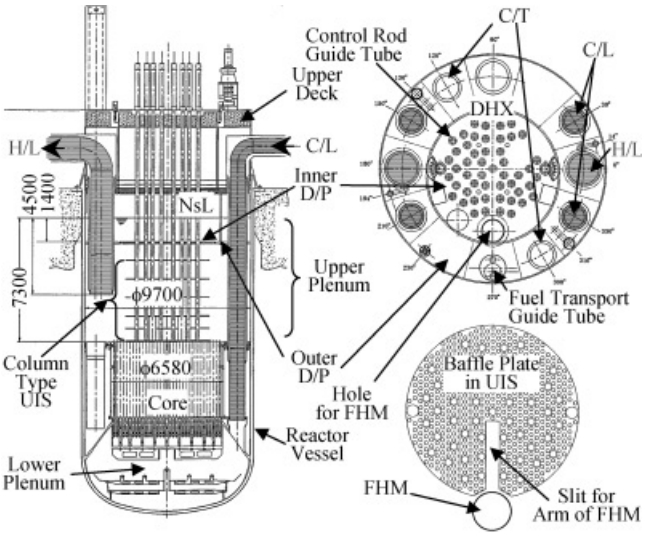

Fig. 1. Reactor vessel of advanced sodium-cooled fast reactor in the design at the end of fiscal 2001.

removes the decay heat in the reactor, are installed in the upper plenum of the reactor vessel. The hot-leg intakes are set at the middle height in the upper plenum. The cold legs pass through the upper plenum. The UIS is set up above the core to insert control rods into the core and to measure subassembly outlet temperature. The UIS consists of six perforated plates and 55 control rod guide tubes. Sodium can flow inside the UIS to increase the mixing volume during a transient (column-type UIS). The lowest perforated plate is named the hold-down plate (HDP), and the other five plates are named the baffle plates. The diameters of the HDP and the baffle plates are ~5000 mm and correspond to the driver core region, excluding the blanket and the reflector regions. The HDP and the baffle plates have the radial slit for the arm of the FHM to get into the UIS. The widths of the slits in the HDP and the baffle plates are 345 and 385 mm, respectively. The HDP and the baffle plates have a hole above each of the fuel subassemblies; the diameter of each hole is slightly larger than the subassembly outlet.

The dipped plates are set at 1400 mm below the free surface to prevent sodium flow from impinging on the free surface. The dipped plates are divided into the inner and the outer ones. The inner dipped plate can rotate with the UIS during the fuel-handling operation. The inner and outer dipped plates consist of double plates to reduce the flow velocity in the gaps.

There are many gaps between the inner and outer dipped plates, between the dipped plate and the components in the upper plenum, and between the dipped plate and the reactor vessel wall to prevent collisions of the components and structural damages because of the flow-induced vibration, thermal expansion, and so on. Therefore, the labyrinths formed like horseshoes or L-shaped

characters are set at the gap region to restrict flow passing through the gaps.

II.B. Experimental Apparatus

The scale of the experimental model is one-tenth. The model scale was decided so as to change geometry easily and find a suitable one, when we considered the design phase of the reactor system early on. Figure 2 shows the bird's-eye view of the one-tenth–scaled experimental apparatus of the reactor vessel upper plenum. Figure 3 shows the top view of the upper plenum. Eguchi[4] showed that the onset condition of gas entrainment was the same velocity condition as in the real reactor through the four scaled models. Therefore, our one-tenth–scaled model can be operated up to the same velocity condition at the core outlet as in the designed reactor. The geometry of the reactor vessel upper plenum was modeled correctly with one-tenth scale, including the inner components. Table I shows the comparisons of dimensions between the experimental apparatus and the upper plenum in the reactor. The diameter of the upper plenum in the experimental apparatus is 1.0 m. In the upper plenum, the UIS, two hot legs, four cold legs, two cold traps, a DHX, a fuel transport guide tube, and the inner and outer dipped plates are set up as well as in the reactor. The dipped plates are modeled as single plates in the experiment to estimate the velocity toward the free surface conservatively. Almost all components in the upper plenum are made of transparent materials, e.g., acrylic resin to visualize flow pattern and to measure local velocity using optical methods. In the reactor design, the widths of the gaps between the dipped plates and every component are 15 to 70 mm. The experimental apparatus has slightly larger-width gaps than those in proportion to the scale (one-tenth) of the reactor. In the reactor design, there is a hole to insert the FHM through the inner dipped plate in the direction of the UIS slit, as shown in Fig. 1. We discuss the effect of the hole on the flow field at the latter half of Sec. III.B. We used the dipped plate without the FHM hole (completely closed) in the beginning of this study.

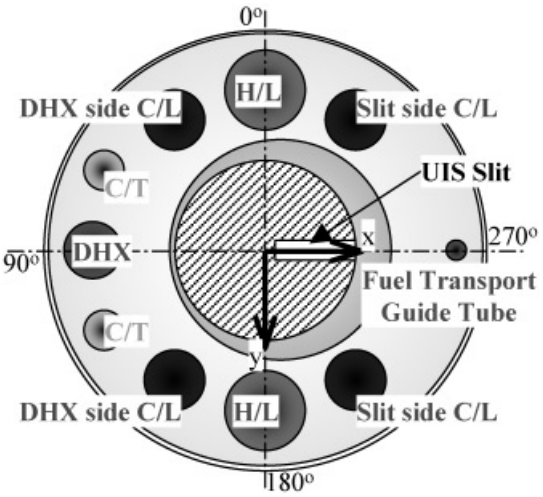

Fig. 3. Top view of the upper plenum in the experimental apparatus.

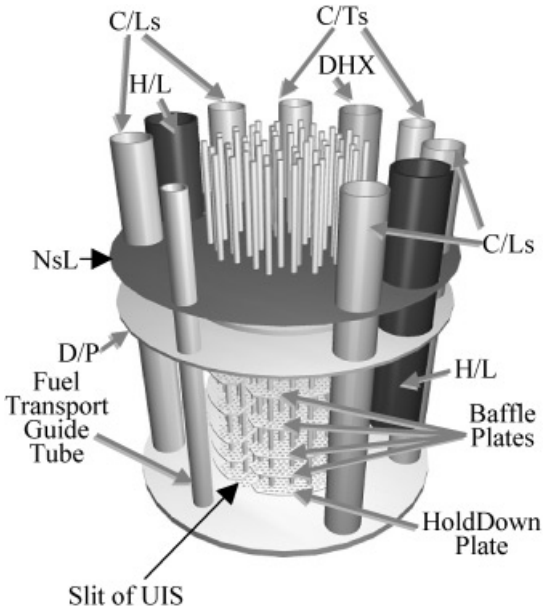

Fig. 2. Bird's-eye view of one-tenth–scaled experimental apparatus of the upper plenum.

II.C. Experimental Conditions

The objective of this study is the flow optimization in the upper plenum of the reactor vessel, e.g., prevention of the gas entrainment at the free surface, cavitations, and flow instability, etc. The experimental apparatus, however, is too small in comparison with the reactor design to evaluate occurrence of the gas entrainment quantitatively, even though flow velocity is equal to that in the reactor. Under the same velocity condition, the Froude number is far from the reactor condition, and the free surface displacement will be enhanced in the small model. Thus, the suppression of the flow velocity toward the free surface is one of the goals in this study.

The flow similarity, including the free surface, is dependent on the Froude number and the Reynolds number. The effect of the Reynolds number on flow field will be small under a larger Reynolds condition.[4] Also, we carried out the experiment in which the velocity was changed to investigate the Reynolds number dependency of flow pattern. Hereby, we confirmed the flow pattern was independent of the Reynolds number in the experiment. Thus, we mainly performed the experiment under the Froude number similarity condition.

TABLE I

Comparisons of Dimensions Between Experimental Apparatus and Reactor

Structural Components	Instrumental Position	Reactor	One-Tenth–Scaled Model	Notes
Reactor vessel	ID[a]	9700[b]	960[b]	Thermal liner (20 mm) is set just inside the reactor vessel wall
Hot leg	PCD[c]	3875	384	OD of protective tube (reactor)
	OD[d]	1487.5	150	
	ID	1282.3	130	
Cold leg	PCD	4035	399	OD of protective tube (reactor)
	OD	1077.2	110	
Cold trap	PCD	3900	390	
	OD	989.5	100	
DHX	PCD	4050	385	
	OD	1269	125	
Fuel transport guide tube	PCD	4315	426.5	
	OD	711.8	60	
Inner dipped plate	Eccentric distance	310	31	Dual dipped plates (reactor)
	OD (upper)	5603.9	550	
	OD (lower)	5321.2		
Outer dipped plate	OD	9520	944	Dual dipped plates (reactor)
Gap of dipped plate − components		30	5	"C"-shaped labyrinth (reactor) Distance of labyrinth − components: 15 mm
Gap of dipped plate − reactor vessel		70	8	"L"-shaped labyrinth (reactor)

[a]Inner diameter.
[b]Measured in millimeters.
[c]Horizontal distance from the center of reactor vessel.
[d]Outer diameter.

The Froude number is defined as follows:

$$\mathrm{Fr} = V/\sqrt{gL} \quad . \tag{1}$$

Here, V is the outlet velocity of the core, and L is the diameter of the reactor vessel. In the experiment under the same Froude number condition, the core outlet velocity is $1/\sqrt{10}$ times smaller than that in the reactor. And the same velocity condition as in the reactor was also examined to see the occurrence of gas entrainment qualitatively. The experimental apparatus used water as working fluid, temperature was 15 to 30°C. The flow rate at the blanket region was set at 5% of total flow rate; flow velocity at the blanket fuel outlet was 12% of that in the driver fuel.

II.D. Techniques of Flow Field Measurement

At first, we performed flow visualization using a tuft method and small-bubble injection method to grasp the qualitative flow pattern in the reactor vessel upper plenum. The visual observation was carried out using a digital video camera (Sony VX2000) and fluorescent lights as a light source. The bubble behavior was affected by buoyancy force because the typical diameter of the bubbles was ~1 mm. Therefore, we used the bubble injection method at the high-velocity region only. Quantitative velocities were obtained using the PIV and the UVP monitor.

The PIV is one of the optical measurements based on image processing techniques to get instantaneous and spatial velocity profile. Recently, the PIV has been applied to the velocity measurement with complex geometry by advances of image processing. Our PIV system was based on a cross-correlation method with subpixel accuracy.[8] And noise reduction techniques[9] for the visualized images were applied to reduce the error velocity vectors near the structures. The laser sheet, generated by a double-pulsed Nd-YAG laser system, was inserted into the apparatus. Nylon particles were used as seeding, and the diameter was ~30 to 50 μm. And a charge-coupled device (CCD) camera, which could capture 30 images per second, was set in the normal direction to the laser

sheet. The pixel number of the camera was 1008 horizontally (H) × 1018 vertically (V), and the size of the image was ~150 mm (H) × 150 mm (V). The spatial resolution of the velocity measurement was 3 mm. The measured region in the model was subdivided, and the images were captured in the multiple regions by moving the CCD camera and the laser sheet. The time interval of the velocity measurement was 0.067 s, and the number of the velocity field data was 300 or 600 (10 or 20 s) at one position. The spatial resolution of the PIV was 3 mm. The accuracy of the PIV measurement was ~0.3 m/s.

The UVP is a noncontact measurement technique of flow velocity based on ultrasound Doppler shift. The emitted ultrasound beam is scattered by the particles and returns to the emitted sensor. The position and velocity information are evaluated, respectively, from the detected time of flight and the Doppler-shift frequency. The nearly instantaneous one-dimensional velocity profile along the beam is obtained. The UVP system could get 1024 data for 40 s and at 128 spatial points along the beam. We applied the UVP to the velocity measurements at the gap of the dipped plate where the PIV was not installed. The spatial resolution of the UVP was 6 mm, corresponding to the diameter of the ultrasound beam. The accuracy of the UVP was ~0.002 m/s.

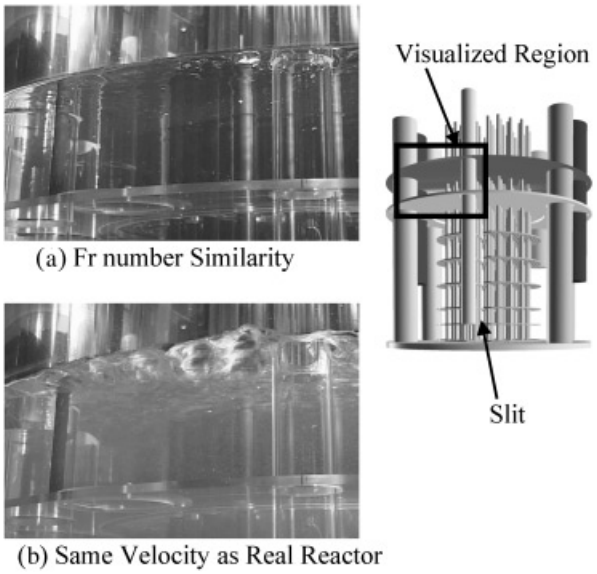

Fig. 4. Visual observation of the free surface in front of the UIS slit.

III. RESULTS AND DISCUSSIONS

III.A. Flow Field in Reactor Vessel Upper Plenum Based on Original Design

At first, we performed the experiment to evaluate the flow field in the geometry based on the design at the end of fiscal 2001.

Figure 4 shows the visual observations of the free surface in front of the UIS slit under the same Froude number and the same velocity conditions as in the designed reactor. The free surface in front of the UIS slit oscillated with the largest magnitude in the entire reactor vessel. In the case of the Froude number similarity, the flow passing through the UIS slit generated only small ripples at the free surface, and the free surface was relatively calm. In the case of the same velocity condition, the upward flow from the UIS slit reached the free surface and lifted up the free surface. The small bubbles due to the ruffled surface were entrained into water intermittently. These bubbles were not entrained continuously and not transported below the dipped plates. These results show that the dipped plate is effective to suppress the gas entrainment. However, it was seen obviously that the flow passing through the UIS slit caused the oscillation of the free surface. This means that the dipped plate is not enough to shut the flow toward the free surface. Thus, it is needed to reduce the velocity through the UIS slit to prevent the gas entrainment. Further reduction of flow velocity through the UIS slit will help a design of the dipped plate, which can permit a larger gap between the penetrating components.

Figures 5a and 5b show the time-averaged velocity vectors at the neighborhood of the UIS slit obtained from the PIV under the Froude number similarity condition. Figure 5a shows the velocity vectors on the side view of the UIS slit and the jet through the slit. Figure 5b shows the velocity vectors on the front view toward the UIS slit. At the region of the UIS slit, the flow exiting the core passed through the slit with high velocity and impinged on the dipped plate. The flow velocity at the undersurface of the dipped plate was 30% at the core outlet. Also, the outer edge of the slit jet was located at the inner gap between the fuel transport guide tube and the dipped plate. The impinging flow easily entered the gap and caused the oscillation of the free surface. After impinging, the flow turned to the horizontal direction and went circumferentially along the undersurface of the dipped plate, as shown in Fig. 5b. As for the core outlet region, excluding the UIS slit, the upward flow from the core passed through the UIS and for the most part went outside in the radial direction along the undersurface of the second baffle plate. This radial flow impinged on the reactor vessel wall and was split into upward and downward flows (see left region in Fig. 5b). Such radial outgoing flow was observed in the circumference of the UIS, except the slit direction. The upward flow inside the UIS did not pass through the fourth baffle plate and exited radially.

It was observed by visualization that the circumferential flow along the undersurface of the dipped plate streamed downward around the hot-leg pipe.

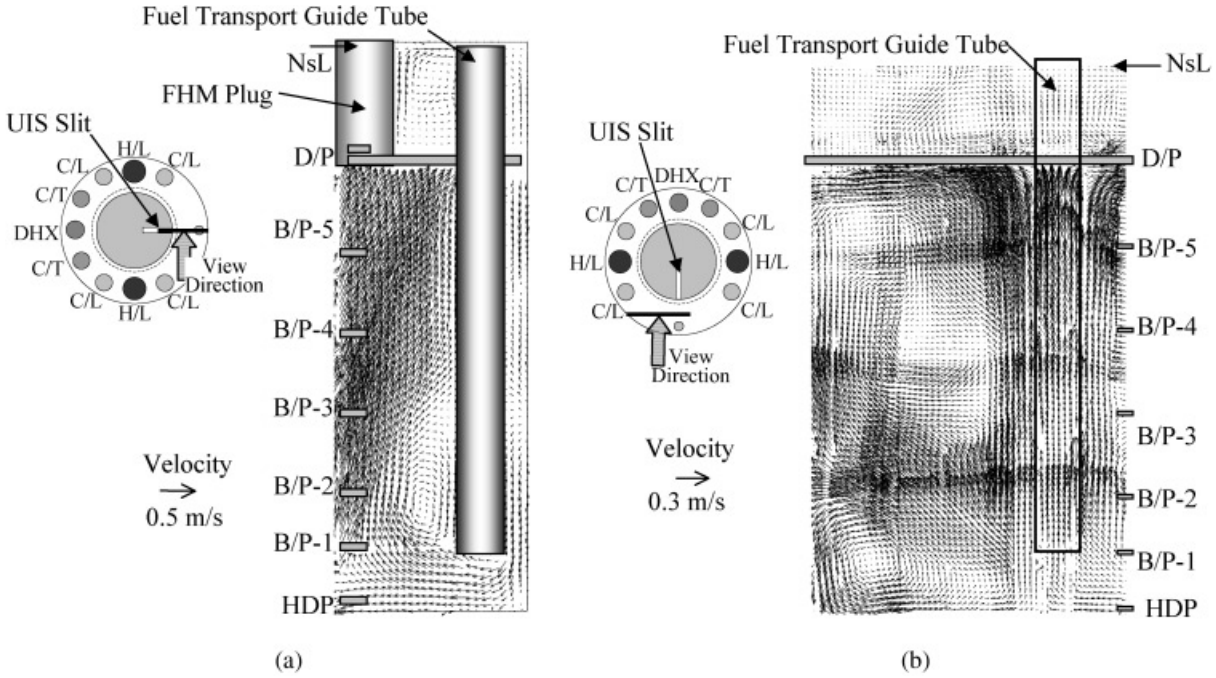

Fig. 5. Time-averaged velocity vectors on (a) the side view of the UIS slit obtained from the PIV and (b) the front view of the UIS slit obtained from the PIV.

Figures 6a through 6d show the time-averaged velocity vectors at the neighborhood of the hot-leg intake obtained from the PIV. Figure 6a shows the velocity vectors on the vertical cross section between the hot leg and the slit side cold leg. Figure 6b shows those on the vertical cross section at the center of the hot leg. Figure 6c shows those on the vertical cross section between the hot leg and the DHX side cold leg. Figure 6d shows those on the vertical cross section between the hot leg and the reactor vessel wall. In the region between the slit side cold leg and the hot leg (see Fig. 6a), a circulation was seen at the height of the hot-leg intake, which was due to the interaction between the downward flow originally coming from the UIS slit and the skewing-up flow coming out from the UIS. As for the flow field at the center cross section through the hot-leg pipe (see Fig. 6b), it was shown that the fluid exiting from the UIS was directly sucked into the hot-leg inlet. In the region between the DHX side cold leg and the hot leg (see Fig. 6c), it was observed that the flow coming out from the UIS promoted the circulation at the height of the hot-leg inlet after impinging on the reactor vessel wall. Also, the downward flow along the hot-leg pipe provided from the DHX side interflowed to this circulation. The downward flow coming from the DHX side was originally outgoing flow from the UIS in the direction of the DHX. Around the DHX, the flow outgoing from the UIS impinged on the reactor vessel wall and the flow was split to the upward and the downward flows. The upward flow reached the dipped plate and finally went toward the hot-leg inlet. In the region between the hot leg and the reactor vessel wall (see Fig. 6d), the downward flow originally coming from the slit (upper right in Fig. 6d) and the upward flow originally coming from the UIS were found at the height of the hot-leg intake. The circulation was generated because of these two flow components, which had the different directions at the neighborhood of the hot-leg intake. Also, the flow coming from the DHX side to the slit side was observed below the hot-leg inlet.

Three circulations were generated at the neighborhood of the hot-leg intake. It was observed that three vortices developed to the vortex cavitations as the inlet velocity of the hot leg increased. Figure 7 shows the visualized image of the vortex cavitations at the neighborhood of the hot-leg intake. The inlet velocity of the hot leg was 7.3 m/s. Three vortex cavitations were observed. One stretched from the reactor vessel wall into the hot leg, and the other two were from both cold legs. It was considered that the vortex cavitations occurred because of the reduction of the pressure at the center of the vortex enhanced by the very high velocity of the hot-leg inlet (9.2 m/s under full-power condition). The cavitations generally have the potential to damage the structural components. The suppression of the cavitations is needed to maintain the structural safety. Static pressure is an important factor to estimate the cavitation. However, there is a large difference in gas pressure above the free surface between the model and the reactor. The cover gas pressure is 0.25 MPa in the reactor design and 0.1 MPa in the model (open to atmosphere). Thus, the

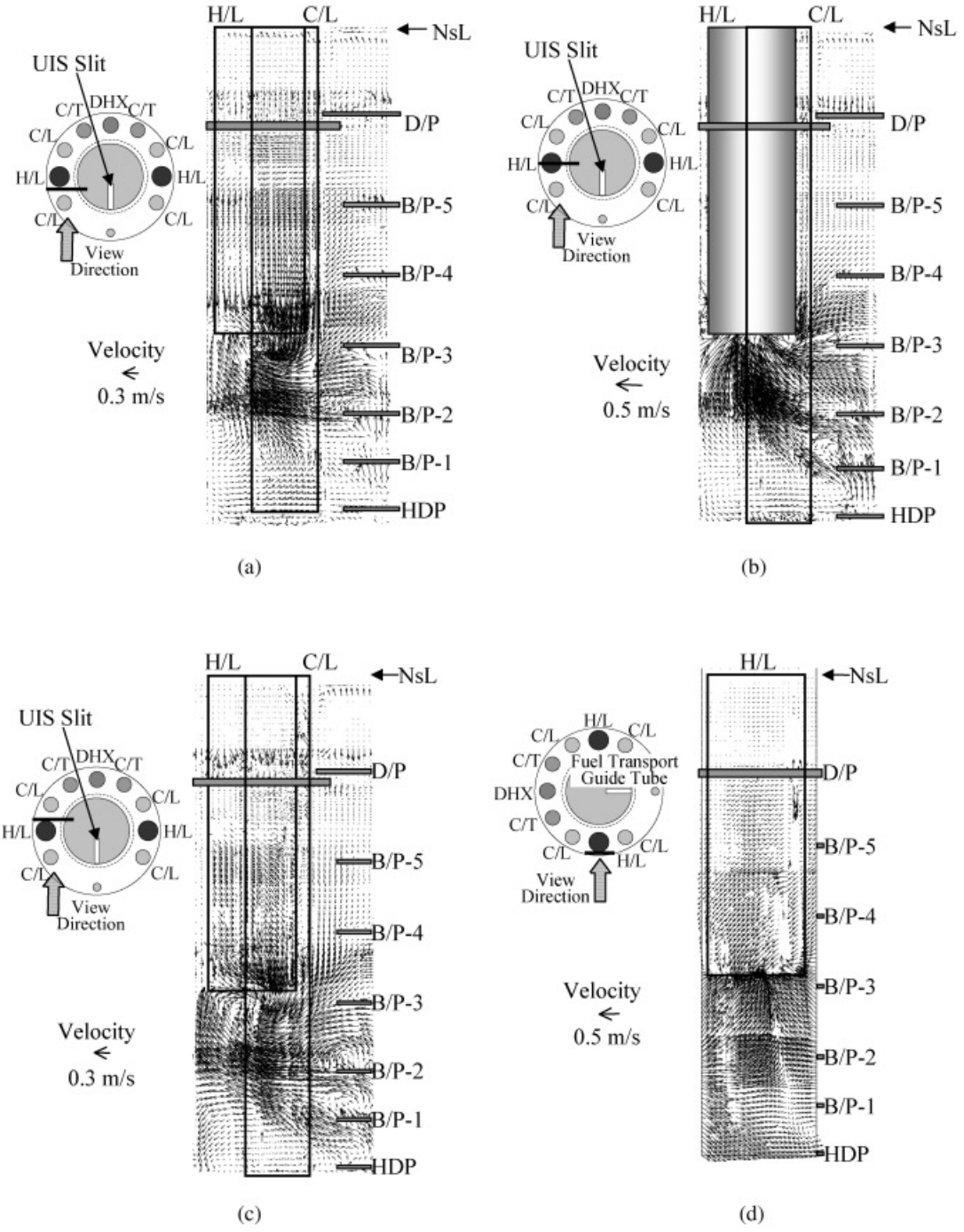

Fig. 6. Time-averaged velocity vectors on the cross sections (a) between the hot leg and the slit side cold leg, (b) through the center of the hot leg, (c) between the hot leg and the DHX side cold leg, and (d) between the hot leg and the reactor vessel wall.

cavitation factor k was used to estimate the onset condition of the vortex cavitation in the reactor. The cavitation factor is defined as follows:

$$k = \frac{P - P_s}{0.5\rho v^2} \quad . \tag{2}$$

Table II shows the cavitation factors at the onsets of the vortex cavitations in the experiment and the cavitation factor under full-power condition in the reactor. The cavitation factor was defined using the average velocity in the hot leg. The cavitation factor in the experiment was ~1.6 times larger than that under the full-power

TABLE II

Cavitation Factors at Onset Conditions of Vortex Cavitations in Experiment and Cavitation Factor Under Full-Power Condition in Reactor

Outbreak Position	Experiment (One-Tenth–Scaled Model)			
	Reactor Vessel–Hot Leg	Slit Side Cold Leg–Hot Leg	DHX Side Cold Leg–Hot Leg	Reactor
Inlet velocities in hot leg (m/s)	4.0	5.0	5.2	9.2
Cavitation factors	12.8	8.0	7.4	8.1

condition of the reactor for the vortex cavitation between the reactor vessel wall and the hot-leg inlet. This means that the vortex cavitation will occur in the reactor. Further, the cavitation factors obtained from the experiment were close to that in the reactor as for the vortex cavitations between both cold legs and the hot-leg inlet. We have to take care of these cavitations also.

We found that the following two points were significant items for the flow optimization in the reactor vessel upper plenum. One is the reduction of the upward velocity passing through the UIS slit, and the other one is the suppression of the vortex cavitations at the hot-leg inlet.

III.B. Flow Optimization in Upper Plenum

First of all, we examined the suppression of vortex cavitations.

In a design of the sump pump, the vortex cavitations have been considered at the intake. The vortex cavitation gives the impeller damage when the cavitation reaches the pump impeller. Some flow control components were investigated to prevent the vortex cavitation by the Japan Society of Mechanical Engineers (JSME) (1984). The JSME standard[10] shows several components, which have the effects to split the flow and to intercept the circulation. One of the components to suppress the cavitation is a vertical rib attached at the wall just behind the pump intake. In our experiment, the vortex cavitation between the reactor vessel wall and the hot-leg inlet occurred under the lowest velocity condition in the hot-leg inlet in comparison with the other vortex cavitations. So we set a vertical rib on the reactor vessel wall near the hot-leg inlet to restrict the rotating flow between the reactor vessel wall and the hot-leg inlet. Figure 8 shows the configuration of the vertical rib. The vertical rib, which is called a "splitter," has a triangle cross section and is $2D_{H/L}$ (= 300 mm) in length. The rib was set on the reactor vessel wall at the nearest position to the hot leg circumferentially and the center was set at the hot-leg

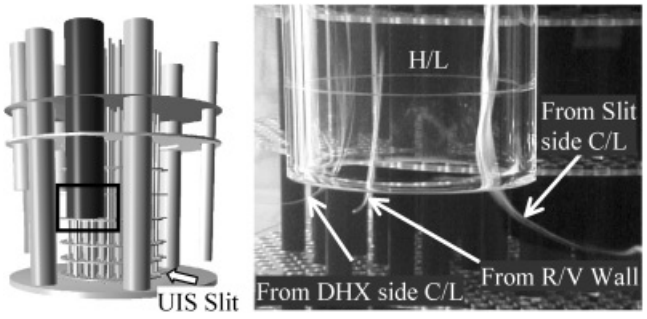

Fig. 7. Visualized image of the vortex cavitations near the hot-leg inlet.

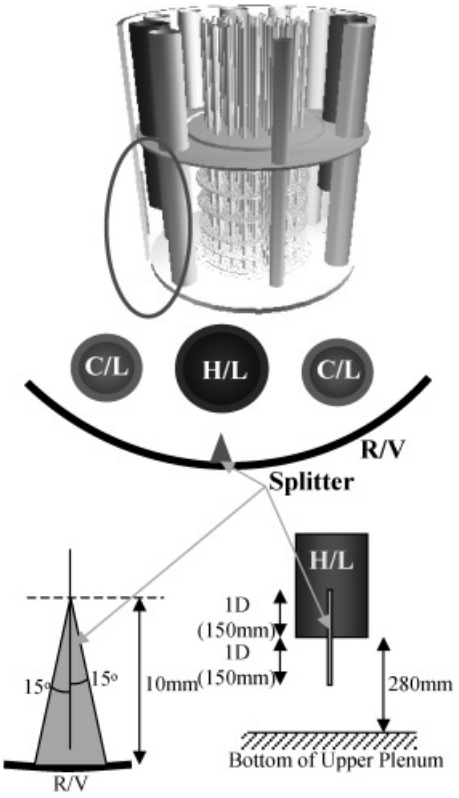

Fig. 8. Configuration of the splitter on the reactor vessel wall.

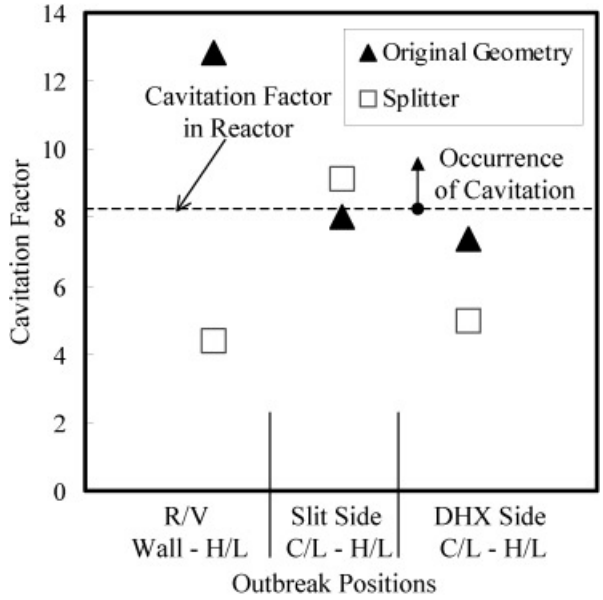

Fig. 9. Cavitation factors based on the average velocity in the hot leg at the onset condition of cavitation.

intake vertically. The rib stuck out about half the distance between the reactor vessel wall and the hot-leg pipe from the wall surface.

Figure 9 shows the comparison of the cavitation factor based on the average velocity in the hot leg at the onset condition of the cavitation with or without the splitter. The cavitation factor is 8.1 under the rated condition in the reactor. It is believed that the vortex cavitation will not occur in the reactor when the cavitation factor in the experiment is smaller than 8.1. In the case of the splitter, the cavitation factor was 4.4, which was smaller than the factor in the reactor at the region between the reactor vessel wall and the hot-leg inlet. As for the vortex cavitations between the DHX side cold leg and the hot-leg inlet, it was shown that the cavitation factors were also decreased by the splitter. At the region between the slit side cold leg and the hot-leg inlet, however, the cavitation was slightly easy to occur in comparison with the original geometry (without the splitter). As described in Sec. III.A, in the original geometry there was inclined downward flow from the UIS slit side dipped plate to the hot-leg intake in the region between the hot leg and the reactor vessel wall. The splitter blocked this transverse flow. This resulted in an increase of downward flow in the slit side region of the hot leg and a decrease in the DHX side region of the hot leg. This is a reason why the splitter influences the onset condition of the vortex cavitations developing from the cold legs.

Figure 10 shows the comparison of the time-averaged velocity vectors between the original geometry and the geometry with the splitter at the region between the reactor vessel wall and the hot-leg pipe. The experimental condition was the Froude number similarity, where the inlet velocity in the hot leg was 2.5 m/s. In the case of the original geometry, the circulation was observed at the hot-leg intake. In the case of the splitter, it was shown that the splitter suppressed the horizontal velocity components above and below the hot-leg inlet, and the vortex was weakened at the height of the hot-leg intake. In other words, the splitter could reduce sufficiently the circulation near the hot-leg inlet and the occurrence of the vortex cavitation between the reactor vessel wall and the hot-leg inlet.

Next, suppression of the UIS slit jet is considered. The FHM will be inserted in the upper plenum to exchange the fuel subassembly. There is a hole in the inner dipped plate to insert the FHM in the design of the reactor.

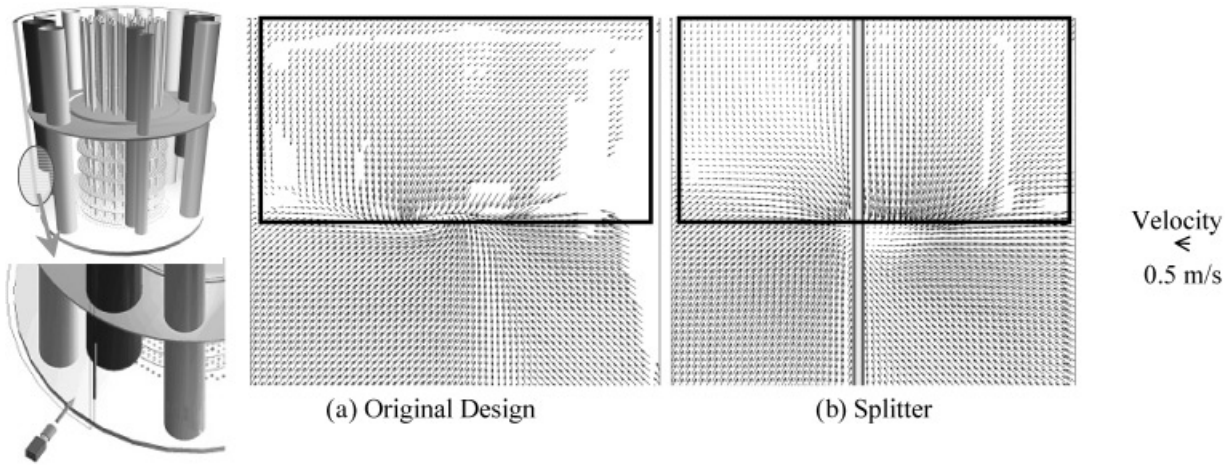

Fig. 10. Comparison of time-averaged velocity vectors between (a) the original geometry and (b) the geometry with the splitter at the region between the reactor vessel wall and the hot leg.

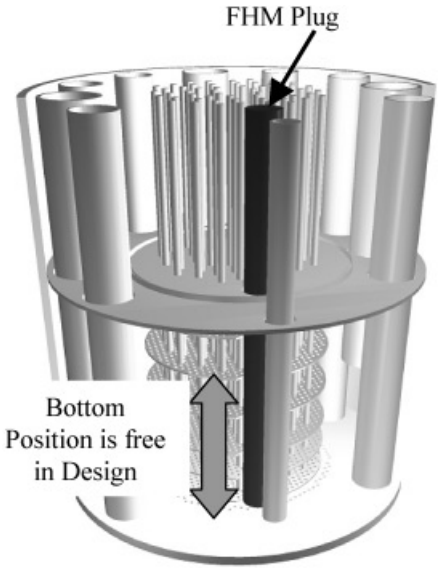

Fig. 11. Concept of the FHM plug.

As shown in Fig. 5a, the flow passing through the UIS slit would directly impinge on the free surface if the hole was not closed under rated condition in the reactor. Therefore, something to close the hole is needed to reduce the flow velocity toward the free surface. In the design, a plug that has nearly the same diameter as the FHM (slightly smaller than the hole) and is suspended by the upper deck is proposed (see Fig. 11). In the design, the length of the plug has flexibility as long as the plug is below the dipped plate. The plug is set in front of the UIS slit. Thus, the plug has the possibility to block the inclined upward flow through the UIS slit to the outer dipped plate when the plug is extended to the middle or lower position in the reactor vessel upper plenum. Also, the plug will affect the vortex cavitations via the downward flow near the hot leg, which was originally coming from the slit jet.

Figure 12 shows the effect of the height of the plug, which fills in the dipped plate hole for the FHM on the flow fields at the vertical cross section through the UIS slit obtained from the PIV. The height of the plug was changed to upper, middle, and lower positions in the reactor vessel upper plenum. The upper, middle, and lower positions meant that the bottom of the plug was set at the heights of the undersurface of the dipped plate, the fourth baffle plate, and the first baffle plate, respectively. The experimental condition was the Froude number similarity. In the case of the upper position of the plug, the flow passing through the slit reached the dipped plate. The flow pattern in this case, of course, was similar to that in the original geometry, which had a completely closed inner dipped plate (see Fig. 5). In the case of the middle position of the plug, it was seen that most of the slit jet struck just the bottom of the plug and was turned to the horizontal direction. Therefore, the slit jet did not reach the dipped plate. In the case of the lower position of the plug, the slit jet flowed along the bottom of the plug in the radial direction. It may be better to insert the plug deeply in the upper plenum to reduce the velocity of the slit jet. However, it was observed that the upward flow

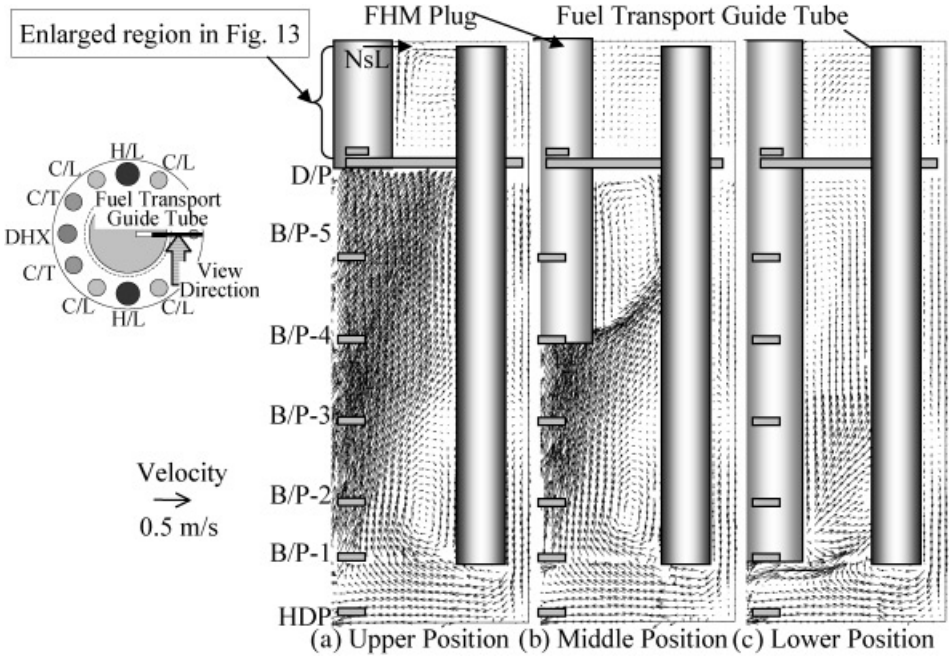

Fig. 12. Effect of the FHM plug height on the flow fields at the cross section through the UIS slit.

along the reactor vessel center side wall of the plug increased in the case of the lower position of the plug.

Figure 13 shows the effect of the plug height on the flow fields above the dipped plate at the vertical cross section through the UIS slit. In the case of the upper position of the plug, the upward flows were found at the outer gap between the plug and the dipped plate and the gap between the dipped plate and the reactor vessel wall. The rising flow, which came from the gap between the plug and the dipped plate, reached the free surface and turned to the horizontal direction along the free surface. In the cases of the middle and the lower positions of the plug, the upward flow weakened in comparison with the case of the upper position of the plug. It was seen that the plug, which was set below the middle position in the upper plenum, reduced the velocity near the free surface.

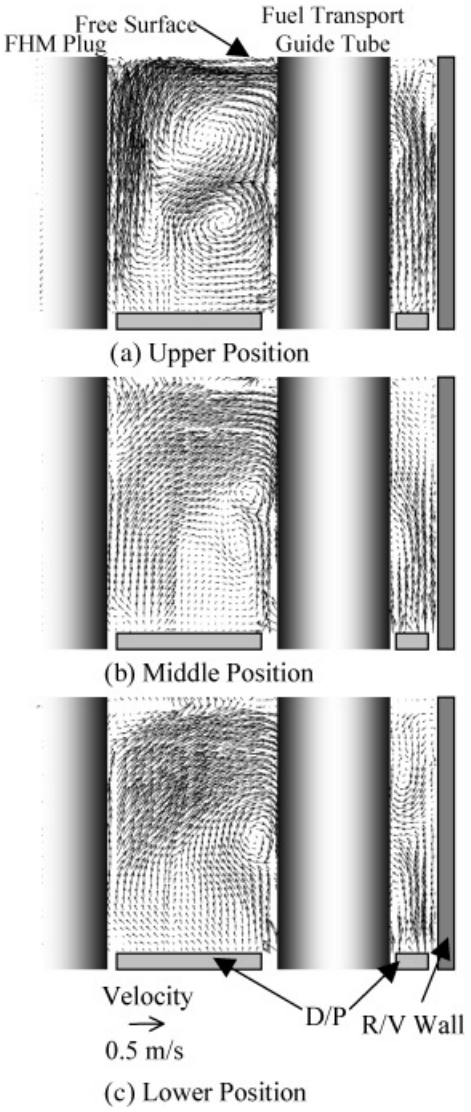

Fig. 13. Effect of the plug height on the flow fields above the dipped plate at the cross section through the UIS slit.

Figure 14 shows the effect of the plug height on the sum of the vertical velocities just above the gap of the dipped plate in front of the UIS slit obtained from the UVP. The sum of the vertical velocities was obtained from adding the time-averaged vertical velocities at the five points in front of the slit; those were the inner and outer gaps between the inner dipped plate and the plug, the inner and outer gaps between the outer dipped plate and the fuel transport guide tube, and the gap between the outer dipped plate and the reactor vessel wall. The sum of the vertical velocities corresponds to the strength of upward flow through the gaps. The sum of the vertical velocities was normalized by that in the original geometry; that was the case of the upper position of the plug. The vertical velocities were measured by the UVP at 5 mm above the dipped plate. The hatching pattern of the bars showed the position of the gap. In the case of the middle and the lower positions of the plug, the flow strength passing through the gaps was ~0.5 times lower than that in the original geometry. The reduction of the upward flow results in the reduction of the downward flow through the dipped plate gaps and the flow velocity near the free surface. The gas entrainment at the free surface will be dependent on the downward velocity. Therefore, it seems that the possibility of gas entrainment decreases in the case of the plug set below the middle position in the upper plenum.

In the case of the upper position of the plug, the rotating vortex with dint, where the vortex string was

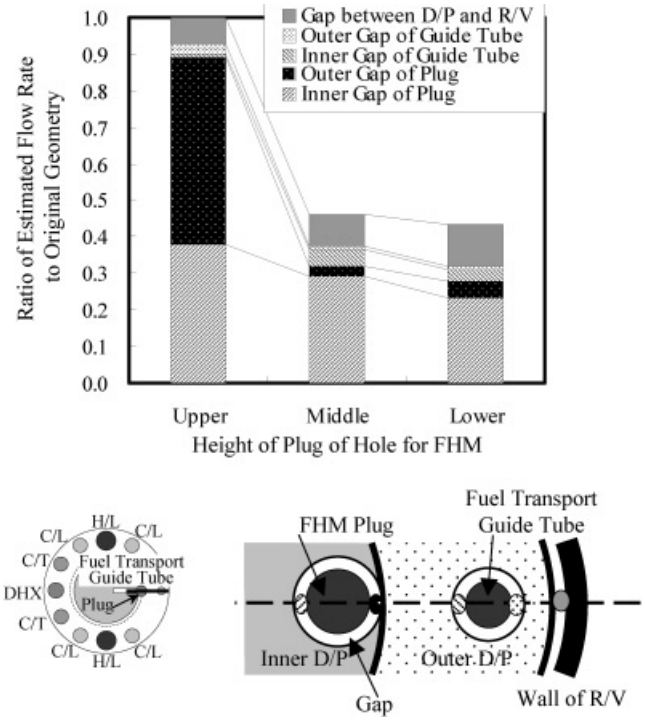

Fig. 14. Effect of the plug height on velocities through the gap of the dipped plate in front of the UIS slit.

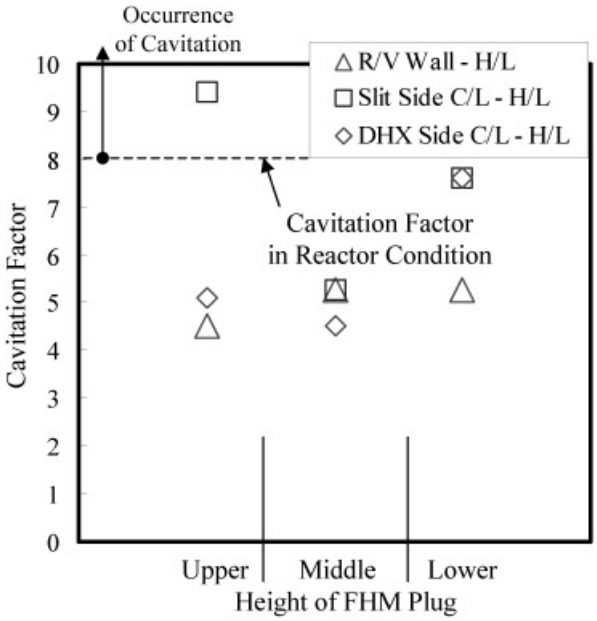

Fig. 15. Effect of the plug height on the cavitation factors at the onset condition of the cavitation.

not stretched below the dipped plate, was observed intermittently at the free surface between the plug and the fuel transport guide tube. In the cases of the middle and the lower positions of the plug, on the other hand, no remarkable vortex was found at the free surface under the conditions from the Froude number similarity to the same velocity as in the reactor. These results showed that the middle or lower position of the plug was better than the upper position from the viewpoint of preventing the gas entrainment.

Figure 15 shows the effect of the plug height on the cavitation factors at the onset condition of the vortex cavitation. In the cases except for the upper position of the plug, it was shown that the obtained cavitation factors were smaller than that in the reactor. In the case of the middle position of the plug, the factors had the largest tolerance. It is desired that the plug is set at the middle position in the upper plenum to suppress the vortex cavitations near the hot-leg inlet.

IV. CONCLUSIONS

An innovative sodium-cooled fast reactor has been investigated as a part of the feasibility study of the FBR cycle system at the Japan Nuclear Cycle Development Institute. Remarkable characteristics of the upper plenum in the reactor vessel are the increase of the velocity and the adoption of a column-type UIS with a radial slit for the FHM. We performed a one-tenth–scale water experiment for the upper plenum of the reactor vessel to evaluate hydraulic phenomena, extract the hydraulic problems, and optimize the flow field. The core outlet velocities in the upper plenum were varied from the Froude number similarity to the same as in the designed reactor.

Gas entrainment at the free surface did not occur within the velocity range in the study. These meant that the dipped plate worked against the gas entrainment. However, the flow passing through the UIS slit impinged on the dipped plate and reached the free surface through the gap of the dipped plate. It was seen obviously that the free surface fluctuated largely in front of the UIS slit. The jet through the slit should be suppressed to prevent the gas entrainment.

Three vortex cavitations were observed at the neighborhood of the hot-leg inlet. One stretched from the reactor vessel wall, and the other two stretched from both cold legs. The cavitation factors, which were obtained from the average velocity in the hot leg at the onset condition of the cavitation, showed that the reactor would have the cavitation. This is needed to suppress the vortex cavitations to keep the structural integrity.

Two hydraulic challenges were pointed out in the upper plenum of the advanced sodium-cooled fast reactor: reduction of the flow passing through the slit of the UIS and suppression of vortex cavitations near the hot-leg inlet.

As for the vortex cavitation from the reactor vessel wall, which was easier to occur, the vertical rib was set on the reactor vessel wall at the closest position to the hot-leg pipe to restrict the rotating flow near the hot-leg inlet.

It was shown that the vortex cavitation between the reactor vessel wall and the hot-leg inlet did not occur under the same cavitation factor (8.1) as in the reactor. The cavitation factor at the onset condition was reduced from 12.8 to 4.4 by the splitter.

To reduce the flow through the UIS slit, an FHM hole in the dipped plate in front of the UIS slit was closed by the plug with the cylindrical shape. The parameter was plug length (height of the bottom of plug). In the case of the middle or the lower plug positions in the upper plenum, the upward flow velocity in the region above the dipped plate was ~0.5 times smaller than that in the original geometry. In these cases, in addition, the vortex cavitation was not broken out anywhere under the same cavitation factor as in the reactor. No gas entrainment occurred under the same velocity condition as in the reactor in all of the cases.

Consequently, there is a chance for this design of the compact reactor vessel to suppress the gas entrainment and vortex cavitation by using flow control devices of the FHM plug and the splitter.

NOMENCLATURE

g = gravity (9.81 m/s^2)

k = cavitation factor

L = representative length (m)

P = pressure (N/m^2)

Ps = saturated vapor pressure of fluid (N/m^2)

Re = Reynolds number

V = velocity (m/s)

ρ = density of fluid (kg/m^3)

ACKNOWLEDGMENTS

The authors appreciate H. Madarame of the University of Tokyo for his encouragement. The authors also are grateful to T. Shiraishi of Mitsubishi Heavy Industries, Ltd., for his advice on the experiment.

REFERENCES

1. H. NODA, "Current Status of Fast Reactor Cycle System in Japan," *Proc. 8th Int. Conf. Nuclear Engineering (ICONE-8)*, Baltimore, Maryland, April 2–6, 2000, American Society of Mechanical Engineers (2000).

2. Y. SHIMAKAWA, S. KASAI, M. KONOMURA, and M. TODA, "An Innovative Concept of the Sodium-Cooled Reactor to Pursue High Economic Competitiveness," *Nucl. Technol.*, **140**, 1 (2002).

3. M. UETA, T. INAGAKI, Y. SHIBATA, K. TARUTANI, and K. OKADA, "The Development of Demonstration Fast Breeder Reactor (DFBR)," *Proc. 3rd Int. Conf. Nuclear Engineering*, Kyoto, Japan, April 23–27, 1995, Vol. 2, p. 771 (1995).

4. Y. EGUCHI, K. YAMAMOTO, T. FUNADA, N. TANAKA, S. MORIYA, K. TANIMOTO, K. OGURA, T. SUZUKI, and I. MAEKAWA, "Gas Entrainment in the IHX Vessel of Top-Entry Loop-Type LMFR," *Nucl. Eng. Des.*, **146**, 373 (1994).

5. T. HIRANUMA, K. YAMAMONO, K. IGASHIGE, M. TAKAKUWA, and H. TOKOI, "Experimental Study of Liquid Properties' Effect on Gas Entrainment Phenomena Induced by Vortices," *Proc. 8th Int. Topl. Mtg. Nuclear Reactor Thermal-Hydraulics*, Kyoto, Japan, September 30–October 4, 1997, Vol. 3, p. 1735 (1997).

6. R. J. ADRIAN, "Particle-Imaging Techniques for Experimental Fluid Mechanics," *Ann. Rev. Fluid Mech.*, **23**, 261 (1991).

7. Y. TAKEDA, "Development of an Ultrasound Velocity Profile Monitor," *Nucl. Eng. Des.*, **126**, 277 (1990).

8. J. SAKAKIBARA, K. HISHIDA, and M. MAEDA, "Measurements of Thermally Stratified Pipe Flow Using Image Processing Techniques," *Exp. in Fluids*, **16**, 82 (1993).

9. N. KIMURA, Y. MIYAKE, A. YASUDA, H. MIYAKOSHI, M. NISHIMURA, A. TOKUHIRO, and H. KAMIDE, "Noise Reduction Techniques for the Particle Image Velocimetry—Application to an Experimental Study on Natural Convection in a Fast Reactor Core," *Proc. 8th Int. Conf. Nuclear Engineering (ICONE-8)*, Baltimore, Maryland, April 2–6, 2000, American Society of Mechanical Engineers (2000).

10. "Standard Method for Model Testing the Performance of a Sump Pump," *JSME Standard*, Maruzen, Tokyo, Japan, Japan Society of Mechanical Engineers (1984) (in Japanese).